RSC Advances

Volume 1 | Number 1 | Jan 2013 | Pages 1–100

RSC Advances

www.rsc.org/advances

ROYAL SOCIETY OF CHEMISTRY

ROYAL SOCIETY OF CHEMISTRY

www.rsc.org/advances

ROYAL SOCIETY
OF CHEMISTRY

RSC Advances

PAPER

Synthesis and chemosensory properties of triphenylamine-substituted conjugated polyfluorene containing terminal di(2-picolyl)amine moiety

Po-Chih Yang,[*] Hua-Wen Wen and Hsiao-Jou He

This paper describes the synthesis of a triphenylamine-substituted alternating conjugated polyfluorene (PFAD) containing a pendant terminal di(2-picolyl)amine (DPA) group through the Heck coupling reaction. We examined the effect of DPA units on the sensory characteristics of fluorescent chemosensors. Photoluminescence titrations demonstrated that PFAD exhibited high sensitivity to Fe^{3+} ions. Furthermore, in a solution of tetrahydrofuran and water, a remarkable change was observed in the fluorescence color of PFAD, which had a Stern-Volmer constant of $1.30 \times 10^3 \, M^{-1}$, from bright blue to dark upon adding Fe^{3+} ions. Because of the considerably high stability constant of the $CN-Fe^{3+}$ complex, the fluorescence of the PFAD solution that was quenched by Fe^{3+} ions recovered upon the addition of trace CN^- anions; the detection limit was as low as $1.08 \times 10^{-5} \, mol \, L^{-1}$. PFAD exhibited a high fluorescence quantum yield (0.73), suggesting that it is a promising material for use in polymeric light-emitting diodes and as a chemosensor.

Introduction

Fluorescent chemosensors are a useful tool for sensing biologically crucial species, such as metal ions and anions, in vitro and in vivo. This is because of the structural simplicity of the chemosensors and the high sensitivity in fluorescence assays.[1] A typical fluorescent chemosensor contains a recognition site linked to a fluorophore, which translates a recognition event into a fluorescence signal.[2] In recent decades, the development of conjugated polymer-derived fluorescent chemosensors for use in detecting metal ions and biological species has attracted increasing attention because the fluorescence properties of the chemosensors respond noticeably to the coupling between the polymer's receptors and target analytes.[3] Moreover, their detection sensitivity is remarkably high for a variety of solution- and vapor-phase analytes.[4] Conjugated polymers, which are used as versatile sensory materials in various environmental applications, offer several crucial advantages over low-molecular-weight compounds. For instance, the chemical signals that are converted into electronic or optical signals when these conjugated polymers bind with an analyte can be transformed and enhanced effectively (i.e., the signals can be amplified).[5] When the conjugated polymers form stable fluorescent ligand-metal ion complexes, the electron charge distribution and molecular conformation of the polymer backbone change because of intra- or intermolecular charge transfer (ICT) and coordination interaction. Since the late 1990s,

fluorescence-amplifying polymers have been extensively employed as sensing materials for detecting metal cations, anions, and pH; for such applications, fluorophores such as fluorene,[6] carbazole,[7] and phenylene ethynylene derivatives[8] are incorporated in the polymer backbone, and receptors such as alkyl ethers,[9] bipyridine,[10] and quinolone[11] are introduced in the main and side chains of the polymers.

Metal ions such as copper, iron, sodium, zinc, and manganese ions are involved in many critical biological processes and are necessary for the survival of all living organisms. They are ubiquitously found in all organisms, almost exclusively as constituents of proteins, including enzymes, storage proteins, and transcription factors.[12] Since its incorporation in fluorescein for the first time in 1996, di(2-picolyl)amine (DPA) has been the most widely used receptor for constructing Zn^{2+} chemosensors.[13] DPA is a classical membrane-permeable chelator with higher selectivity for Zn^{2+} than for alkali- and alkaline-earth metal ions, such as Ca^{2+}, Mg^{2+}, K^+, and Na^+. The secondary amine nitrogen atom of DPA not only serves as an appropriate reaction site that is linked to various fluorophores but is also an effective signal transduction sponsor that responds to the binding events through photoinduced electron transfer (PET) or ICT. Many studies have used DPA units as recognition sites, and in biological and environment systems, the choice of ligand has been demonstrated to have a marked influence on the detection of metal ions.[14] More recently, Xu et al. reported the combination of an amide-containing DPA receptor and a naphthalimide fluorophore for detecting Zn^{2+}.[15] This DPA receptor displayed excellent selectivity for Zn^{2+} over most of the competitive transition and heavy metal ions with an enhanced fluorescence (22-fold enhancement) and a red-shift in emissions from 483 to 514 nm.

Department of Chemical Engineering and Materials Science, Yuan Ze University, Chung-Li, Taoyuan City 32003, Taiwan. E-mail: pcyang@saturn.yzu.edu.tw; Fax: +886 3 4559373; Tel: +886 3 4638800.

RSC Advances Accepted Manuscript

Pu et al. synthesized an unsymmetrical photochromic diarylethene with a DPA unit.[16] When Zn^{2+} was added, the fluorescence intensity of diarylethene increased, and an evident color change from black to bright blue occurred. Bao et al. demonstrated that a DPA-substituted rhodamine B derivative (RBDPA) exhibited high sensitivity to and high selectivity for Al^{3+} among metal cations in an ethanol–H_2O solution.[17] Furthermore, using fluorescence microscopy experiments, they demonstrated that the RBDPA can be used as a fluorescent probe for detecting Al^{3+} in living cells. Li et al. prepared a new polyfluorene (P2) bearing DPA moieties to develop sensitive and selective CN^- chemosensors.[18] They demonstrated that Cu^{2+}, Hg^{2+}, Cd^{2+}, Fe^{3+}, Ni^{2+}, and Al^{3+} could quench the fluorescence of P2. Huo et al. synthesized a water-soluble Fe^{3+} ratiometric fluorescent sensor by encapsulating a donor–acceptor dye 4-formacyl-triphenylamine into silica cross-linked micellar nanoparticle with a detection limit of 4 ppm.[19]

In our previous study, we demonstrated that introducing a triphenylamine (TPA) unit in the main chain of terpyridine-substituted conjugated polyfluorene enhanced the fluorescence sensing performance of conjugated polyfluorene because of the efficient interaction of the specific TPA-linked terpyridine unit with protons, solvents, and metal ions.[20] In this study, we synthesized a DPA-substituted alternating conjugated polymer (PFAD) through the Heck coupling reaction. The PFAD consisted of alternating fluorene and TPA units in the main chain along with pendant DPA ligands that are attached to the vinyl group of the 4-phenyltriphenylamine unit; the ligands were used as recognition sites. The objective of this study was to examine the effect of a DPA unit on the sensory characteristics of fluorescent chemosensors. Additionally, substituting the 4'-(4-styrylphenyl)triphenylamine unit within the polymer was expected to enhance the cation quenching sensitivity because of the increase in the distance of energy transfer migration between the receptors on the polymer chain. In the present system, the PFAD exhibited a highly selective response and rapid recognition to Fe^{3+} ions, with a Stern-Volmer constant (K_{sv}) of 1.30×10^3 M^{-1}. In addition, the resultant polymer–Fe^{3+} complex exhibited markedly selective fluorescence restoration when cyanide ions (CN^-) were added, rendering the polymer a promising material for high-potential chemosensory applications.

Experimental section

Materials

Synthetic routes for the target TPA-based monomer (2) and DPA-substituted intermediate (3) are shown in Scheme 1. The intermediate, tris(4-bromophenyl)amine (1), was synthesized following previously reported procedures.[21] All of the reagents and organic solvents were purchased from Acros, Aldrich, and Alfa Chemical Co. and used without further purification. All solvents were of analytical grade, and were dried with appropriate drying agents, calcium hydride or sodium, then distilled under reduced pressure and stored over 4 Å molecular sieves before use. Synthetic routes for the target conjugated polymers (PFA and PFAD) are shown in Scheme 2.
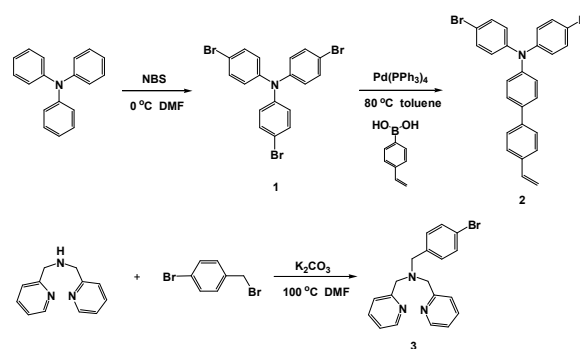

Scheme 1 Synthetic routes of monomer 2 and intermedium 3.

Measurements

^1H NMR (400 MHz) spectra were recorded on a Bruker AMX-400 FT-NMR, and chemical shifts were reported in δ units (ppm) downfield relative to the chemical shift of tetramethylsilane (TMS). Elemental analysis was performed on a Heraeus CHN–O rapid elemental analyzer. Weight-average molecular weight (M_w) and polydispersity index (PDI) of the polymers were measured with a gel permeation chromatograph (GPC), model CR4A from Shimadzu, using tetrahydrofuran (THF) as an eluent and the rate of elution was 1.0 ml min^{-1}; the instrument was calibrated with a polystyrene standards (1000–136000 g/mol). Thermogravimetric analysis (TGA) was performed under nitrogen atmosphere at a heating rate of 20 K/min using a Perkin Elmer TGA-7 thermal analyzer. Thermal analysis was performed using a differential scanning calorimeter (Perkin Elmer DSC 7) at a scanning rate of 20 K/min under nitrogen atmosphere. UV/visible absorption spectra were obtained using a Jasco V-670 spectrophotometer and photoluminescence (PL) spectra were measured using an OBB Quattro II fluorescence spectrophotometer. Fluorescence quantum yields (Φ_{PL}s) of compounds in solution using poly(9,9-dihexylfluorene) (PF) ($\lambda_{ex} = 350$ nm) as the standard were estimated at room temperature by the dilution method (1.1×10^{-3} wt%, assuming a quantum yield of 0.55). All Φ_{PL}s of polymers are relative to that of PF. Cyclic voltammograms were recorded with a voltammetric analyzer (model CV-50W from BAS) at room temperature under nitrogen atmosphere with a scanning rate of 100 mV/s. The measuring cell comprised a polymer-coated ITO as the working electrode, an Ag/AgCl electrode as the reference electrode, and a platinum wire electrode as the auxiliary electrode. The electrodes were immersed in acetonitrile containing 0.1 M tetrabutylammonium perchlorate (n-Bu)$_4$NClO$_4$ as the electrolyte. The energy levels were calculated using the ferrocene (FOC) value of –4.8 eV with respect to vacuum level, which is defined as zero.

Synthesis of monomer

Synthesis of 4''-(4-vinylphenyl)-4,4'-dibromotriphenylamine (2). To a solution of 1 (2.0 g, 4.15 mmol), 4-vinylbenzeneboronic acid (0.245 g, 1.66 mmol), tetrakis(triphenylphosphine) palladium [Pd(PPh$_3$)$_4$] (0.096 g, 0.083 mmol) and aliquat 336 (0.05 g) in
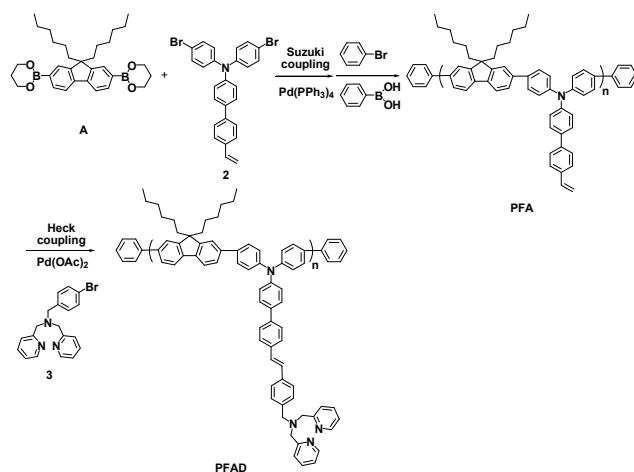
Scheme 2 Synthetic routes of conjugated polymers (PFA and PFAD).

toluene (10 ml) was dissolved in 2 M aqueous potassium carbonate (K_2CO_3) solution (6 ml) and ethanol (6 ml). The solution was then stirred at 80 °C under nitrogen atmosphere. After stirring for 48 hr, the solution was poured into an excess of methanol solution, and then the crude product was collected by filtration and further purified by column chromatography using *n*-hexane as eluent to give 2. Yield: 32.0%. ^{1}H-NMR (CDCl$_3$, δ in ppm): 5.27-5.29 (dd, 1H, CH=C), 5.80-5.82 (dd, 1H, CH=C), 6.74-6.81 (dd, 1H, CH=C), 6.94-6.97 (d, 4H, aromatic, Ar-H), 7.08-7.11 (d, 2H, aromatic, Ar-H), 7.36-7.39 (d, 4H, aromatic, Ar-H), 7.45-7.55 (d, 6H, aromatic, Ar-H). Anal. Calcd. (%) for $C_{26}H_{19}Br_2N$: C, 61.81; H, 3.76; N, 2.77. Found: C 62.02; H, 3.70; N, 2.86.

Synthesis of 4-bromobenzyl-di(2-picolyl)amine (3). A mixture of di(2-picolyl)amine (0.996 g, 5.0 mmol), potassium carbonate (K_2CO_3) (1.04 g, 7.5 mmol), potassium iodide (1.0 mg, 0.006 mmol) and N,N-dimethylformamide (DMF, 30 ml) was heated at 100 °C for 0.5 h, and then 4-bromobenzyl bromide (1.5 g, 6.0 mmol) was added dropwise into the above system with stirring for 24 h. After cooling to room temperature, the mixture was poured into a stirred of ice water and then extracted with dichloromethane. The organic layer was successively washed with water twice, dried over anhydrous magnesium sulfate and concentrated under reduced pressure. Yield: 62.1%. ^{1}H-NMR (acetone-d_6, δ in ppm): 3.67 (s, 2H, CH$_2$), 3.77 (s, 4H, CH$_2$), 7.20 (t, 2H, aromatic, Ar-H), 7.42 (d, 2H, aromatic, Ar-H), 7.48 (d, 2H, aromatic, Ar-H), 7.60 (d, 2H, aromatic, Ar-H), 7.73 (t, 2H, aromatic, Ar-H), 8.48 (d, 2H, aromatic, Ar-H). Anal. Calcd. (%) for $C_{19}H_{18}BrN_3$: C, 61.97; H, 4.89; N, 1.14. Found: C, 61.54; H, 4.86; N, 1.18.

Synthesis of conjugated polymers

The synthesis of a TPA-substituted polyfluorene (PFA) was carried out using a palladium-catalyzed Suzuki coupling reaction. The general synthetic procedures for the PF derivative are described as follows: To a solution of predetermined amount monomers in toluene was added with aqueous potassium carbonate (2M) and ethanol. The mixture was degassed and exchanged with nitrogen for three times, and a catalytic amount of tetrakis(triphenylphosphine)

palladium [Pd(PPh$_3$)$_4$] (1.5 mol %) was added in one portion under nitrogen atmosphere. The solution was then stirred at 90 °C under nitrogen atmosphere. After stirring for 24 hr, the end groups, bromobenzene and phenylbornoic acid, were then capped by refluxing subsequently for 6 h each. After cooling, the solution was poured into a large amount of methanol solution, and then the crude polymers were collected by filtration and further purified by extraction with acetone for 24 h in a Soxhlet apparatus to remove monomers and catalyst residues.

Synthesis of poly[2,7-(9,9-dihexylfluorene)-*alt*-4''-(4-vinylphenyl)-4,4'-triphenylamine] (PFA). The composition of the reactants were 9,9-dihexylfluorene-2,7-diboronic acid bis(1,3-propanediol) ester (A) (0.502 g, 1.0 mmol), 2 (0.505 g, 1.0 mmol), toluene (6.5 ml), Pd(PPh$_3$)$_4$ (0.0346 g, 0.03 mmol), 2 M aqueous K_2CO_3 solution (6 ml) and aliquat 336 (20.0 mg); end-capping by bromobenzene (50.0 mg, 0.32 mmol), and phenylboronic acid (50.0 mg, 0.41 mmol). Yield: 81.2%. T_g = 169.1 °C. ^{1}H NMR (CDCl$_3$, δ in ppm): 0.66-1.32 (m, CH$_2$ and CH$_3$), 1.96-2.10 (br, CH$_2$), 5.21-5.27 (br, CH=C), 5.68-5.77 (br, CH=C), 6.65-6.79 (br, CH=C), 7.24-7.81 (m, Ar-H and vinyl). Anal. Calcd. (%) from feed ($C_{25}H_{32}$)($C_{26}H_{19}N$): C, 90.40; H, 7.53; N, 2.07. Found: C, 88.67; H, 6.88; N, 2.21.

Synthesis of poly[2,7-(9,9-dihexylfluorene)-*alt*-4''-(4-di(2-picolyl)amino-styrylphenyl)-4,4'-triphenylamine] (PFAD). The synthesis of PFAD was carried out using a palladium-catalyzed Heck coupling reaction, using palladium acetate (Pd(OAc)$_2$) as the catalyst. To a solution of PFA (100.0 mg), 3 (3.68 g, 10.0 mmol), Pd(OAc)$_2$ (0.045 g, 0.2 mmol) and tri-*p*-tolylphosphine (0.304 g, 1 mmol) was added with a solution of triethylamine (1.518 g, 15.0 mmol) dissolved in 20 ml DMF. The solution was then stirred at 100 °C under nitrogen atmosphere. After stirring for 48 hr, the solution was poured into a large amount of methanol solution, and then the crude polymers were collected by filtration and further purified by extraction with acetone for 24 h in a Soxhlet apparatus to remove compound 3 and catalyst residues. Yield: 25.4%. T_g = 138.3 °C. ^{1}H NMR (CDCl$_3$, δ in ppm): 0.62-0.85 (br, CH$_2$), 0.94-1.15 (m, CH$_3$), 1.35-1.49 (m, CH$_2$), 1.90-2.08 (br, CH$_2$), 3.45-3.50 (br, NCH$_2$), 3.69-3.78 (br, NCH$_2$), 7.12-7.80 (m, Ar-H and vinyl). Anal. Calcd. (%) from feed ($C_{25}H_{32}$)($C_{45}H_{36}N_4$): C, 87.14; H, 6.33; N, 5.81. Found: C, 86.52; H, 6.57; N, 5.45.

Fluorescent titration of polymer

Fluorescent titration experiments were carried out in THF solution. The chloride salts of Ca^{2+}, Mg^{2+}, Mn^{2+}, Zn^{2+}, Ni^{2+}, Fe^{3+}, K^+, Cu^{2+}, Fe^{2+}, Ag^+, Al^{3+}, Ba^{2+}, Pb^{2+}, Hg^{2+}, Cr^{3+}, and Co^{3+} (5.0×10^{-3} M) were dissolved in distilled water. Titration was done by adding the metal ion solution to a test tube with polymer solution. The final concentration of polymer was 1.1×10^{-3} wt%. Titration of the metal ions was terminated until no change in the fluorescence intensity was observed. The percentage of water in THF was approximately 1.0 %. The Stern-Volmer constant (K_{sv}) was estimated according to following equation:

$$(I_o/I) = 1 + K_{sv}[Q] \qquad (1)$$

where I_o and I are the intensity of PL spectrum without and with a quencher, respectively, K_{sv} is the Stern-Volmer constant (quenching coefficient), and $[Q]$ is the concentration of the quencher ions. The stabilization of PFAD-Fe^{3+} complex was investigated in the presence
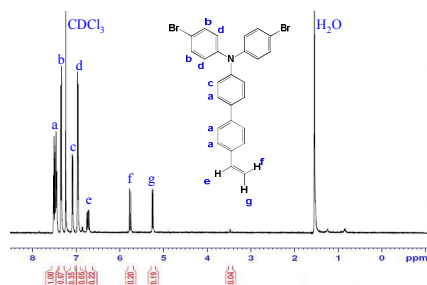
Please do not adjust margins
RSC Advances
Page 4 of 9
View Article Online
DOI: 10.1039/C5RA20562J
Paper
RSC Advances

Fig. 1 ^{1}H NMR spectrum of monomer 2.

of some anions, including Cl$^-$, Br$^-$, I$^-$, NO$_3^-$, NO$_2^-$, HSO$_4^-$, and CN$^-$ (1.0×10^{-5} M).

Results and discussion

Synthesis of monomer and polymers

The synthetic routes of the required TPA-based monomer (2) and DPA intermediate (3) are presented in Scheme 1. The target monomer 4''-(4-vinylphenyl)-4,4'-dibromotriphenylamine (2) was prepared by reacting tris(4-bromophenyl)amine (1) with 4-vinylbenzeneboronic acid at 80 ^{o}C. The reaction was a Suzuki coupling reaction involving Pd(PPh$_3$)$_4$ as a catalyst, and the yield of monomer 2 was 32.0%. We prepared 4-bromobenzyl-di(2-
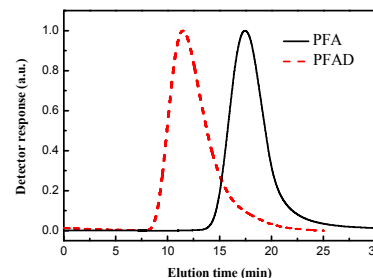

Fig. 3 GPC traces of PFA and PFAD.

picolyl)amine (3) in 62.1% yield by using the nucleophilic substitution reaction of DPA with 4-bromobenzyl bromide in the presence of K$_2$CO$_3$. The chemical structures and composition of the synthesized compounds were confirmed by ^{1}H NMR spectroscopy and elemental analysis. Fig. 1 displays the ^{1}H NMR spectrum of monomer 2 in CDCl$_3$. The spectrum exhibits characteristic chemical shifts of the doublet proton signals (d; H$_a$, H$_b$, H$_c$, and H$_d$) and the vinyl group doublet of doublets (dd; H$_e$, H$_f$, and H$_g$) at 6.94–7.55 and 5.27–6.81 ppm, respectively. The ^{1}H NMR spectrum of compound 3 displays characteristic chemical shifts of the pyridyl doublet (–NCH–) and methylene singlet (–NCH$_2$–) at 8.48 and 3.67–3.77 ppm, respectively.

Poly[2,7-(9,9-dihexylfluorene)-alt-4''-(4-vinylphenyl)-4,4'-tri-phenylamine] (PFA) was prepared using Suzuki coupling polymerization and was reacted in toluene at 90 ^{o}C using 1:1 molar ratio of monomer A to monomer 2 (Scheme 2). PFAD was prepared using the Heck reaction; PFA and excess of 3 were used as the reactants, and Pd(OAc)$_2$ was the catalyst. PFAD was successfully synthesized, as confirmed by the apparent disappearance of vinyl protons at 5.21–6.79 ppm (Fig. 2b) and the appearance of methylene protons (H$_a$ and H$_b$) at 3.45–3.78 ppm, which is attributable to the DPA substituents (–NCH$_2$–). Other aromatic and vinyl protons appeared at 7.12–7.80 ppm. Finally, the ^{1}H NMR spectrum of PFAD exhibited peaks at approximately 1.90–2.08, 1.35–1.49, 0.94–1.15, and 0.62–0.85 ppm, which were assigned to the aliphatic protons labeled H$_c$, H$_e$, H$_f$, and H$_d$, respectively, of the hexyl groups of the fluorene unit (Fig. 2b). The ^{1}H NMR spectrum in combination with
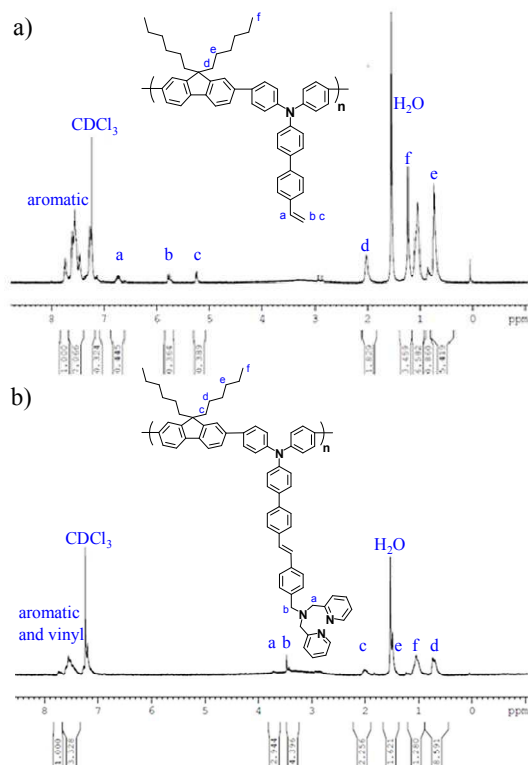

Fig. 2 ^{1}H NMR spectra of (a) PFA and (b) PFAD.

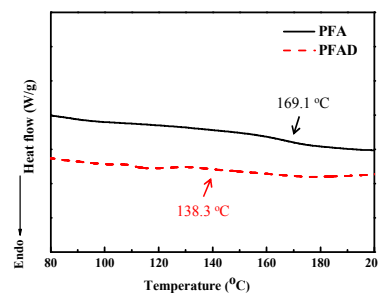**Fig. 4** DSC traces of polymers at a heating rate of 10 ^{o}C min^{-1} under nitrogen atmosphere.

Table 1 Molecular weights and thermal properties of polymers

No.	Yield (%)	$M_w{}^a$ (g mol^{-1}) ($\times 10^4$)	PDI^a	$T_g{}^b$ (^{o}C)	$T_d{}^c$ (^{o}C)
PFA	81.2	3.32	3.20	169.1	438.5
PFAD	25.4	4.60	3.14	138.3	421.6

^{a} M_w and PDI of the polymer were determined by gel permeation chromatography using polystyrene as a standard in THF. ^{b} Glass transition temperature was observed using DSC under N_2 at a heating rate of 10 ^{o}C/min. ^{c} The onset temperature of weight loss measured using TGA.

elemental analysis data confirmed the successful synthesis of PFAD.

The weight-average molecular weights (M_ws) of PFA and PFAD were 3.32 $\times$ 10^4 and 4.60 $\times$ 10^4 g mol^{-1}, respectively, and the corresponding PDIs were 3.20 and 3.14, respectively (Table 1). The GPC traces of PFA and PFAD are illustrated in Fig. 3. GPC analysis demonstrated that the numbers of repeating unit (n) of the main chain was 48.8 and 47.5 for PFA and PFAD, respectively, indicating that 97.3% of DPA was attached to the vinyl group of TPA in the polymer chain. Both polymers exhibited high solubility in common solvents such as THF, CHCl$_3$, and toluene. As displayed in Table 1, the glass transition temperatures (T_g) of PFA and PFAD were approximately 169.1 ^{o}C and 138.3 ^{o}C, respectively (Fig. 4). The thermal decomposition onset temperatures (T_d) were in the range of 421.6–438.5 ^{o}C. The polymers had residual weights greater than 49.7 % at 800 ^{o}C, indicating high thermal stability.

Optical and electrochemical properties

Typical absorbance and emission spectra for PFA and PFAD in the THF solution are summarized in Table 2 and Fig. 5. PFA and PFAD demonstrated strong absorbance maxima at approximately 380 nm, which results from a π-π* electronic transition of the conjugated polymer backbone. Furthermore, for both polymers, the polymer absorbance maxima of the film state were blue-shifted by approximately 4–10 nm relative to those of the solution state, and broad absorption bands in the range of 445–500 nm and spectral

Table 2 Optical properties of conjugated polymers

No.	UV-vis $\lambda_{max}{}^a$ sol'n (nm)	UV-vis λ_{max} film (nm)	PL $\lambda_{max}{}^b$ sol'n (nm)	PL λ_{max} film (nm)	Stokes Shift^c	$\Phi_{PL}{}^d$
PFA	380	370, 467	436, 482s	463, 486s	93	0.46
PFAD	380	376, 457s	437, 510s	415, 482	39	0.73

^{a} Measured in THF solution (1.1 $\times$ 10^{-3} wt%). ^{b} The excitation wavelengths were 350 nm for all polymers. Superscript s means the wavelength of the shoulder. ^{c} Stokes shift = PL$_{(film)}$/nm – UV$_{(film)}$/nm. ^{d} These values of quantum yield were measured using PF as a standard (assuming a quantum yield of 0.55).
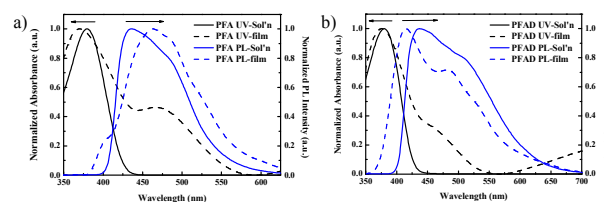
Fig. 5 Normalized UV-vis absorption and PL spectra of (a) PFA and (b) PFAD in THF solution (solid line) and in film (dotted line).

band-widths (full-width at half maximum) of approximately 85–110 nm were observed. The absorption bands and spectral bandwidths were associated with aggregate formation resulting from intra- or interchain interactions. The emission spectra of the polymers in the solution exhibited the maxima and a shoulder at approximately 436 and 482–510 nm, respectively. We attributed this observation to the different vibrational-rotational levels of the excited states and ground electronic states. The Stokes shifts of PFA and PFAD were 93 and 39 nm, respectively (Table 2), implying that donor-acceptor interactions occurred between the polymer backbone and DPA acceptor group. The Φ_{PL} values of PFA and PFAD, estimated using PF as the reference (Φ_{PL} = 0.55), were 0.46 and 0.73, respectively, suggesting that the introduction of the terminal DPA group in the polymer side chain enhanced Φ_{PL}; we attributed this enhancement to the resonance effect of the 4'-(4-styrylphenyl)triphenylamine groups.

The cyclic voltammetry data and molecular orbital energy values of the polymers in CH$_2$Cl$_2$ are illustrated in Table 3 and Fig. 6. The highest occupied molecular orbital (HOMO) and lowest unoccupied molecular orbital (LUMO) energy levels were evaluated according to the equations E_{HOMO} = $-(E_{ox}$ + 4.8) eV and E_{LUMO} = E_{HOMO} + $E_g{}^{opt}$, where E_{ox} is the onset oxidation potential regarding the standard ferrocene/ferrocenium (FOC) redox system. The optical band gaps ($E_g{}^{opt}$) were determined based on the onset absorption wavelength. The onset oxidation potential of PFA was 0.28 V; however, the onset oxidation potential for PFAD exhibited a slight shift to 0.26 V. We attributed the decrease in the oxidation potential of PFAD to the charge delocalization of the extended π-system of the TPA and DPA groups. The estimated HOMO energy levels of PFA and PFAD were –5.08 and –5.06 eV, respectively. The optical band gaps ($E_g{}^{opt}$), determined from the onset of absorption in the solution state, were 2.92 eV (424 nm) for PFA and 2.88 eV (430 nm) for PFAD. Consequently, the estimated LUMO energy levels of PFA and PFAD were –2.16 and –2.18 eV, respectively.

Ion sensing properties

The TPA-based PF, PFAD, is a multifunctional material consisting of a conjugated polymer backbone and a pendant DPA unit, and PFAD is used as a chemical sensor for cations and as an emission material for electroluminescent devices. Fig. 7 describes the effect of PFAD complexation with various metal ions (Ag$^+$, Al^{3+}, Ba^{2+}, Ca^{2+}, Cu^{2+}, Fe^{2+}, Fe^{3+}, K$^+$, Mg^{2+}, Mn^{2+}, Ni^{2+}, Pb^{2+}, Li$^+$, Zn^{2+}, Hg^{2+}, Cr^{3+}, and Co^{3+}) on the PL spectra of PFAD in a THF–H$_2$O solution. The PL intensity of the solution decreased considerably upon adding Ag$^+$, Cu^{2+}, Fe^{2+}, Fe^{3+}, Ni^{2+}, Zn^{2+}, or Pb^{2+} ions (Fig. 7a), indicating that

Table 3 Optical and electrochemical properties of polymers

No.	UV-vis λ_{onset}[a] (nm)	E_{ox} (onset)[b] (V)	E_{HOMO}[c] (eV)	E_{LUMO}[d] (eV)	E_{g} (opt)[e] (eV)
PFA	424	0.28	−5.08	−2.16	2.92
PFAD	430	0.26	−5.06	−2.18	2.88

[a] Onset wavelength of polymers in absorption spectra. [b] The cyclic voltammograms of polymers in CH_2Cl_2 at a scanning rate of 100 mV/s (vs FOC^+/FOC). [c] $E_{HOMO} = -(E_{ox} + 4.8)$ eV. [d] $E_{LUMO} = E_{HOMO} + E_{g}$ (opt). [e] The optical band gaps were determined from the onset of absorption in CH_2Cl_2 (E_{g} (opt) = 1240/λ_{onset}).

these metal ions led to the efficient fluorescence quenching of the polymer chain. In particular, PFAD was quenched almost completely by Fe^{3+} ions, indicating its high selectivity toward this cation. The quenching mechanism of polymers can be attributed to the initial photoinduced energy transfer (PET) occurring in a collision (dynamic quenching) between the excited fluorophore and metal ions. We also attributed the quenching behavior to strong cation binding between Fe^{3+} ions and the DPA chelating groups; the binding results from the effective energy transfer migration between the receptors and polymer chains. Thus, PFAD could be used in polymer chemosensors for detecting metal ions.
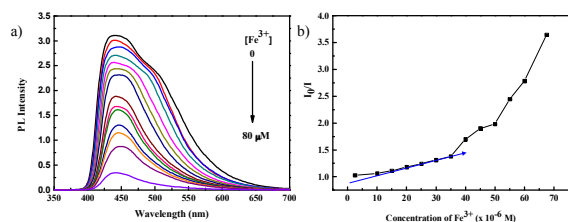
Fig. 7b displays the PL response profiles (i.e., I_o/I) of PFAD in the presence of various metal ions with an ion concentration of 5.0 × 10^{-5} M. In the presence of Al^{3+}, Ba^{2+}, Ca^{2+}, K^+, Li^+, Mg^{2+}, Mn^{2+}, Hg^{2+}, Cr^{3+}, and Co^{3+}, the fluorescence spectra of PFAD exhibit a slight decreases in intensity, and the complexation of metal ions does not induce any shift in the emission peak. We found that PFAD demonstrated high sensitivity toward Fe^{3+}, which was reflected by a marked change in the fluorescence from bright blue to dark blue in the THF–H_2O solution (Fig. 7c). These results indicate that the charge density and diameter of the metal ions, quenching mechanism (i.e., collisional quenching, energy transfer, charge transfer reactions, or photochemistry), and chelating capability of DPA ligands considerably influence the fluorescence quenching behavior, thereby leading to the observed variation in chelating ability. Consequently, the smaller diameter (1.28 Å) and higher charge (1.83) of Fe^{3+} might have a higher electron-accepting capability and consequently lead to more stable complexes, and these two factors (i.e., diameter and charge) might play a vital role in determining the coordination
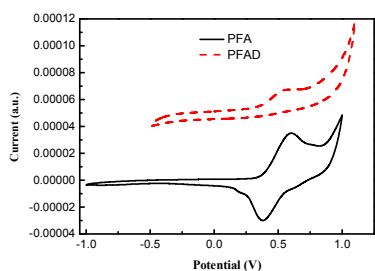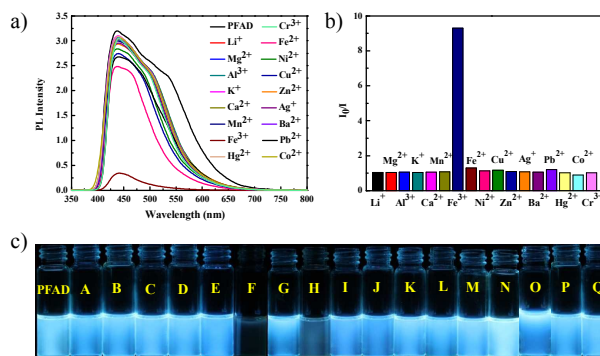
Fig. 7 (a) Photoluminescence spectra, (b) PL response profiles, and (c) fluorescence colors of PFAD in the presence of various cations (excitation: 350 nm). Insert in (c): (A) Li^+ (0.58), (B) Mg^{2+} (0.58), (C) Al^{3+} (0.59), (D) Ca^{2+} (0.59), (E) Mn^{2+} (0.56), (F) Fe^{3+} (0.04), (G) K^+ (0.58), (H) Fe^{2+} (0.38), (I) Ni^{2+} (0.48), (J) Cu^{2+} (0.46), (K) Zn^{2+} (0.52), (L) Ag^+ (0.53), (M) Ba^{2+} (0.58), (N) Pb^{2+} (0.44), (O) Hg^{2+} (0.58), (P) Co^{2+} (0.58), and (Q) Cr^{3+} (0.56). The values in brackets are their corresponding quantum yields (Φ_{PL}s) after adding cation. The Φ_{PL} of PFAD in THF solution was 0.73.

strength of the Fe^{3+} ions accompanying DPA units.[22] The five electrons (Fe^{3+}: d^5 electron configuration) may be present as two orbitals occupied by pairs of electrons and one having single occupancy, leading to the inner-orbital complex, which was more stable than the other host/metal complexes.[23] The Φ_{PL} values of PFAD in the presence of Fe^{2+} and Fe^{3+} ions decreased by approximately 47.9% (i.e., from 0.73 to 0.38) and 94.5% (i.e., from 0.73 to 0.04), respectively.

To quantitatively evaluate the fluorescence sensitivity of the polymer toward Fe^{3+}, the PL intensities and Stern-Volmer constant (K_{sv}) of PFAD for various concentrations of Fe^{3+} ions were measured at room temperature. As displayed in Fig. 8a, the fluorescence intensities decreased with an increase in the Fe^{3+} concentration. When the Fe^{3+} concentration exceeded 3.5 × 10^{-5} M, the slope of the Stern-Volmer plot exhibited a noticeable upward turn, (i.e., static quenching), which we attributed to strong DPA chelation to the transition metal ions. The K_{sv} value of PFAD at low concentrations of Fe^{3+} ions (below approximately 3.5 × 10^{-5} M) was 1.30 × 10^3 M^{-1}; furthermore, the estimated detection limit was as low as 1.08 × 10^{-5} M, indicating that PFAD is a selective and sensitive Fe^{3+} cation probe. We concluded that the synthesized polymer (PFAD) detected the presence of Fe^{3+} ions on the basis of its fluorescence "turn-off" characteristics associated with efficient energy transfer within the polymer backbone and DPA moiety.

To determine whether the PFAD−Fe^{3+} complex could be used as an anion selective probe, the response of the complex toward anions (Br^-, Cl^-, I^-, NO_3^-, NO_2^-, HSO_4^-, and CN^-) was investigated (Fig. 9a). The PL response profiles (i.e., I/I_o) of PFAD−Fe^{3+} complexes in the presence of CN^- anions with a concentration of 1.0 × 10^{-5} M are provided in Fig. 9b. These data illustrate that the PL intensity of the

Fig. 6 Cyclic voltammograms of polymers in CH_2Cl_2 at a scanning rate of 100 mV/s.
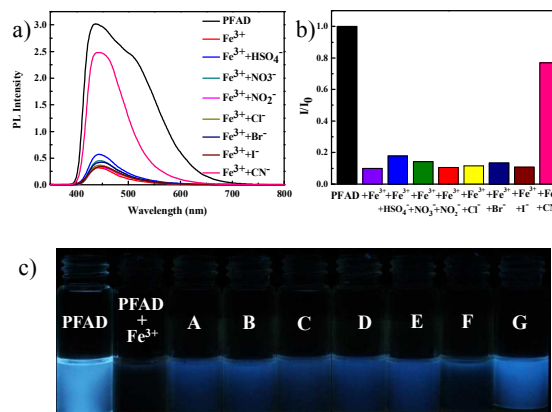
Please do not adjust margins

Fig. 8 (a) PL spectra of PFAD and (b) Stern-Volmer plot of PL quenching with various concentrations of Fe^{3+} ion. Concentration of polymer: 1.1×10^{-3} wt% in THF.

Fig. 9 Photoluminescence spectra, (b) PL response profiles, and (c) fluorescence colors of PFAD–Fe^{3+} in the presence of various anions. Insert in (c): (A) HSO_4^- (0.07), (B) NO_3^- (0.06), (C) NO_2^- (0.04), (D) Cl^- (0.05), (E) Br^- (0.05), (F) I^- (0.04), and (G) CN^- (0.36). The values in brackets are their corresponding quantum yields (Φ_{PL}s) after adding anion. The Φ_{PL} of PFAD–Fe^{3+} was 0.04.

PFAD−Fe^{3+} complex increased considerably upon adding CN^- ions, whereas complexation with other anions did not induce any obvious shift in the emission peak because of the poor coordination of Fe^{3+} with these anions. However, in the presence of HSO_4^-, the PL spectrum of the PFAD−Fe^{3+} complex exhibited a slight increase in the PL intensity. The complex demonstrated a remarkably selective fluorescence "turn-on" behavior when CN^- ions were added, indicating that CN^- ions could effectively coordinate with Fe^{3+} instead of PFAD. This finding is attributed to the high stability of the Fe^{3+}–CN^- complex.[24] Consequently, the fluorescence of PFAD was revived by the transformation of the PFAD−Fe^{3+} complex (quenched, "turn-off") to a free polymer (revived, "turn-on"). When the concentration of CN^- was 1.0×10^{-5} M, the fluorescent intensity recovered up to 77.0% of the original intensity, whereas adding HSO_4^- led to a recovery of up to 18.5% of the original intensity. Thus PFAD−Fe^{3+} complex is a sensitive CN^- sensor. In addition, the Φ_{PL} values of the PFAD−Fe^{3+} complex in the presence of CN^- and HSO_4^- ions increased from 0.04 to 0.36 (approximately 46.4% of the original Φ_{PL} of PFAD) and from 0.04 to 0.07 (approximately 4.3%), respectively. The fluorescence response to various anions corresponded to different emission colors (Fig. 9c).

Conclusions

We synthesized and characterized a DPA-containing polyfluorene using the Heck reaction. We evaluated the effect of DPA units on the PL property of the polymer on the sensory characteristics of fluorescent chemosensor. The synthesized polymers exhibited moderate thermal stability with thermal decomposition temperature (5% weight loss) greater than 410.7 °C, suggesting that the introduction of TPA groups in the polymer enhanced intermolecular interaction. Our results suggest that PFAD exhibited high selectivity toward Fe^{3+} ions ("turn-off") with a Stern-Volmer constant (K_{sv}) of 1.30×10^3 M^{-1}. Moreover, the PFAD−Fe^{3+} complex displayed remarkably selective fluorescence recovery ("turn-on") upon the addition of CN^- ions. These results indicate that PFAD has high potential for use in practical view to selective requirements for environmental and biomedical applications.

Acknowledgements

Notes and references

1 (a) R. Y. Tsien, *Fluorescent and Photochemical Probes of Dynamic Biochemical Signals inside Living Cells*, ed. A. W. Czarnik, American Chemical Society, Washington, D. C., 1993, Vol. 538, pp. 130–146; (b) M. Saleem and K. H. Lee, *RSC Adv.*, 2015, **5**, 72150–72287.
2 A. P. de Silva, H. Q. N. Gunaraten, T. Gunnlaugsson, A. J. M. Huxley, C. P. McCoy, J. T. Rademacher and T. E. Rice. *Chem. Rev.*, 1997, **97**, 1515–1566.
3 (a) D. T. McQuade, A. E. Pullen and T. M. Swager, *Chem. Rev.*, 2000, **100**, 2537–2574; (b) Y. Hu, Z. Zhao, X. Bai, X. Yuan, X. Zhang and T. Masuda, *RSC Adv.*, 2014, **4**, 55179–55186.
4 P. D. Barata and J. V. Prata, *ChemPlusChem*. 2014, **79**, 83–89.
5 S. W. Thomas, G. D. Joly and T. M. Swager, *Chem. Rev.*, 2007, **107**, 1339–1386.
6 J. M. Yu and Y. Chen, *Macromolecules*, 2009, **42**, 8052–8061.
7 R. S. Juang, P. C. Yang, H. W. Wen, C. Y. Lin, S. C. Lee and T. W. Chang, *React. Funct. Polym.*, 2015, **93**, 130–137.
8 S. J. Dwight, B. S. Gaylord, J. W. Hong and G. C. Bazan, *J. Am. Chem. Soc.*, 2004, 126, 16850–16859.
9 A. Balamurugan, V. Kumar and M. Jayakannan, *Chem. Commun.*, 2014, **50**, 842–845.

10 X. Liu, X. Zhou, X. Shu and J. Zhu, *Macromolecules*, 2009, *42*, 7634–7637.

11 S. J. Ou, Z. H. Lin, C. Y. Duan, H. T. Zhang and Z. P. Bai, *Chem. Commun.*, 2006, *42*, 4392–4394.

12 M. I. Hood and E. P. Skaar, *Nat. Rev. Microbiol.*, 2012, *10*, 525–537.

13 R. P. Haugland, *Handbook of Fluorescent Probes and Research Chemicals*, ed. M. T. Z. Spence, Molecular Probes, Eugene, OR, 6th edn, 1996, pp. 530–540.

14 (a) Z.-H. Xu, H.-W. Wang, X.-F. Hou, W.-L. Xu, T.-C. Xiang and C.-C. Wu, *Sens. Actuators, B*, 2014, *201*, 469–474 ; (b) Q. Hu, Y. Tan, M. Liu, J. Yu, Y. Cui and Y. Yang, *Dyes Pigments*, 2014, *107*, 45–50; (c) K. Komatsu, Y. Urano, H. Kojima and T. Nagano, *J. Am. Chem. Soc.*, 2007, *129*, 13447–13454.

15 Z. Xu, K. Baek, H. Kim, J. Cui, X. Qian, D. R. Spring, I. Shin and J. Yoon, *J. Am. Chem. Soc.*, 2010, *132*, 601–610.

16 S. Cui, G. Liu, S. Pu and B. Chen, *Dyes Pigments*, 2013, *99*, 950–956.

17 X. Bao, Q. Cao, Y. Xu, Y. Gao, Y. Xu, X. Nie, B. Zhou, T. Pang and J. Zhu, *Bioorgan. Med. Chem.*, 2015, *23*, 694–702.

18 X. Lou, Y. Zhang, S. Li, D. Ou, Z. Wan, J. Qin and Z. Li, *Polym. Chem.*, 2012, *3*, 1446–1452.

19 F. Gai, T. Zhou, Y. Liu and Q. Huo, *J. Mater. Chem. A*, 2015, *3*, 2120–2127.

20 R. S. Juang, H. W. Wen, M. T. Chen and P. C. Yang, *Sens. Actuators, B*, SNB-D-15-03241, 2015.

21 (a) J. Louie and J. F. Hartwig, *J. Am. Chem. Soc.*, 1997, *119*, 11695–11696; (b) H. J. Lee, J. Sohn, J. Hwang and S. Y. Park, *Chem. Mater.*, 2004, 16, 456–465.

22 J. E. House, *Inorganic Chemistry*, Academic Press, Elsevier, Burlington, MA, 2008.

23 Y. Cui, Q. Chen, D. D. Zhang, J. Cao and B. H. Han, *J. Polym. Sci. Part A: Polym. Chem.*, 2010, *48*, 1551–1556.

24 (a) Q. Zeng, P. Cai, Z. Li, J. Qin and B. Z. Tang, *Chem. Commun.*, 2008, 1094–1096; (b) X. Lou, D. Ou, Q. Li and Z. Li, *Chem. Commun.*, 2012, *48*, 8462–8477.

RSC Advances Accepted Manuscript

Graphical abstract

Metal ions

Fe^{3+} or Fe^{2+}

Blue
Strong fluorescent

Colorless
Weak fluorescent or quenching

PFAD Li⁺ Mg²⁺ Al³⁺ Ca²⁺ Mn²⁺ Fe³⁺ K⁺ Fe²⁺ Ni²⁺ Cu²⁺ Zn²⁺ Ag⁺ Ba²⁺ Pb²⁺ Hg²⁺ Co²⁺ Cr³⁺